Axial-resolution in depth from focus digital holography

van Rooij, J.; Kalkman, Jeroen

DOI
10.1117/12.2270295

Publication date
2017

Document Version
Final published version

Published in
Digital Optical Technologies 2017

Axial-resolution in depth from focus digital holography

Joseph van Rooij, Jeroen Kalkman

Joseph van Rooij, Jeroen Kalkman, "Axial-resolution in depth from focus digital holography," Proc. SPIE 10335, Digital Optical Technologies 2017, 103351F (26 June 2017); doi: 10.1117/12.2270295

SPIE.

Event: SPIE Digital Optical Technologies, 2017, Munich, Germany

Axial-resolution in depth from focus digital holography

Joseph van Rooij[a] and Jeroen Kalkman[a]

[a]Delft University of Technology, Lorentzweg 1, 2628 CJ Delft, The Netherlands

ABSTRACT

We use digital holography to quantify surface topography of rough objects in full-field. We calculate the variance of the intensity image as a focus metric over a set of reconstruction distances for each pixel, which results in a focus metric curve. The distance where the variance peaks is an estimate for the depth. First we analyze the lateral resolution of this method using the Talbot effect and argue that sub-mm axial resolution is feasible. Then, using a Michelson setup without magnifying optics or lateral scanning we experimentally demonstrate that sub-mm FWHM width of the focus curve can be achieved. This is significantly better than what was previously reported using digital holography and could make this technique useful for characterising objects in art and machine vision.

Keywords: Digital holography, metrology, Talbot effect, depth from focus

1. INTRODUCTION

Surface metrology and absolute distance measurement are essential in many applications; for example in the field of geosciences, remote sensing aims to reconstruct the surface topology and track changes of the earth surface over time. On a much smaller scale, optical measurement of surface metrology has become vital in many manufacturing methods.[1] Depth from focus digital holography (DFF-DH) is a technique that combines the advantages of focus variation microscopy (FVM) and digital holographic microscopy (DHM), namely the short acquisition time of DHM (no scanning is needed) with the ability to reconstruct topographies with large discontinuities or rough surfaces in FVM. In contrast to ordinary imaging where the focus is varied by changing the position of the lens, in DH the image can be calculated at any plane. The DFF-DH approach is an image processing approach that estimates the surface location from the optimum of a metric is calculated from the digitally reconstructed image. For 3D objects the image plane depends on the distance of every part of the object to the camera. By reconstructing the image of the object at different depths, the degree of focus of a particular region in the image reconstruction (calculated with a focus measure) encodes the depth of the object.[2] Because one can reconstruct the complete wave-field at any depth from a single digitally captured hologram, this method does not need lateral or axial scanning and has no fundamental limit regarding the depth range that can be measured other than the coherence length of the light source. This was first used within the context of digital holography by Ma et al. (2004),[3] who recovered object depth for every part of the object in this way from a digital hologram. In this paper we show how the depth resolution of DFF-DH depends on experimental setup parameters. In the next section, we first give an overview of the basic principles of DFF-DH and a theoretical framework to analyze the precision. Then, we compare our framework with simulations where we show that sub-mm resolution is possible. We then experimentally demonstrate the sub-mm resolution in the results section.

2. THEORY

In digital holography the image is numerically calculated from an interferogram, instead of it being formed optically with a lens. For an explanation of the basic principles of digital holography, we refer the reader to Schnars and Jueptner (2005).[4] The degree of focus in the reconstructed image depends on the reconstruction distance and therefore encodes the distance of the object to the sensor. In contrast to ordinary imaging where the focus is varied by changing the position of the lens, in DH the image can be calculated at any plane. Since

Further author information: (Send correspondence to J. van Rooij)
J. van Rooij: E-mail: j.vanrooij@tudelft.nl

Digital Optical Technologies 2017, edited by Bernard C. Kress, Wolfgang Osten,
H. Paul Urbach, Proc. of SPIE Vol. 10335, 103351F · © 2017 SPIE
CCC code: 0277-786X/17/$18 · doi: 10.1117/12.2270295

the degree of focus is at its maximum when z_1=z_0 (reconstruction distance equals recording distance), one needs to quantify the degree of focus with a focus measure and find the optimum value as a function of reconstruction distance. For each pixel in the object-image we can repeat this process and calculate its distance to the sensor plane z_0. Other more sophisticated ways of estimating the depth from the focus metric data have also been applied in FVM,[1] but are not implemented in this paper. The degree of focus in the image as a function of reconstruction distance z_1 depends on the numerical aperture (NA) of the imaging system. In digital holography, the NA is inversely proportional to the recording distance and proportional to the dimensions of the sensor.

2.1 Focus measure

The degree of focus is quantified using image based metrics. These metrics are calculated from the image and have their maximum when the image is in focus, and decrease rapidly when the image is out of focus. Different focus metrics exist, see for example Tian et al. (2007) for an overview.[5] Variance is a focus measure that is simple to calculate, and has been proven to be a good depth measure.[6] The variance of a a digital image I of n x m pixels is given by:

$$\sigma^2 = \frac{1}{n\,m}\sum_{i=1}^{n}\sum_{j=1}^{m}(I(i,j)-\overline{I})^2 \tag{1}$$

where $\overline{I}$ is the mean intensity of the image. In order to derive an analytic model for the variance as a function of reconstruction distance, we will use the integral form which is given by

$$\sigma^2 = \int\int (I(x,y)-\mu)^2 \mathrm{d}x\,\mathrm{d}y\,, \tag{2}$$

where μ is the mean of the image and is given by

$$\mu = \int\int I(x,y)\mathrm{d}x\,\mathrm{d}y \tag{3}$$

2.2 Depth Estimation

The focus metric for a planar object as a function of reconstruction distance is a curve that peaks when the reconstruction distance equals the recording distance. Here we derive an expression for a reflecting planar object with a uniform spatial frequency spectrum and random phase for each spatial frequency. First we consider a single spatial frequency at recording distance z_0 as input to the holographic imaging system, which we reconstruct at reconstruction distance z_1. In order to keep the expressions concise we will consider a one dimensional input, although a generalization to two dimensions is straightforward. Neglecting the finite extent of the aperture, we consider an object described by the reflection

$$t_n = \frac{1}{2}[1 + m\cos(2\pi n\xi/L) + \phi_n] \tag{4}$$

where ϕ_n is a random phase term, n/L is the spatial frequency and m is an amplitude factor and ξ is the lateral spatial coordinate in the input plane. In principle n can be any number, although in practice it is an integer value due to discrete sampling. The reconstructed holographic wavefield is calculated using Fresnel diffraction according to the treatment of Goodman (1996)[7] and is given by

$$U_n(\xi,z_1) = \frac{2 + 2me^{-\frac{i\pi\lambda n^2(z_0+z_1)}{L^2}}\cos\left(\frac{2\pi n\xi}{L} + \phi_\mathrm{n}\right)}{4N}\,. \tag{5}$$

The intensity of the reconstructed wavefront is given by:

$$I_n(\xi, z_1) = \frac{1}{4N^2}\left(m\cos\left(\frac{2\pi n\xi}{L} + \phi_{\mathrm{n}}\right) + 2\cos\left(\frac{\pi\lambda n^2(z_0+z_1)}{L^2}\right)\right) \\ m\cos\left(\frac{2\pi n\xi}{L} + \phi_{\mathrm{n}}\right) + \frac{1}{4N^2}\,. \tag{6}$$

This reduces to $|t_n|^2$ for distances

$$z_1 = -z_0 + \frac{2L^2 n}{\lambda}\,, \tag{7}$$

which means that the input grating is replicated at fixed distances, also called "self-imaging". This occurs for periodic inputs in general and is a manifestation of the Talbot effect[7] appearing in holographic reconstruction. The variance for one spatial frequency as a function of reconstruction distance is then found by calculating the integral in one dimension (Eq. (2)) over the integration range 0 to L, which yields

$$\sigma_n^2(z_1) = a + b\,\cos\left(\frac{2\pi\lambda n^2(z_0+z_1)}{L^2}\right) \tag{8}$$

where m is assumed to be equal to one, and

$$a = \frac{9L\left(2L^2 - 4L + 3\right)}{128N^4} \tag{9}$$

and

$$b = \frac{L}{16N^4} \tag{10}$$

For every spatial frequency n/L the variance is thus periodic as a function of reconstruction distance z_1. For this reason we will refer to such a curve as a Talbot curve. We now assume that the object is composed of many spatial frequencies:

$$t_N = \frac{1}{N}\sum_{n=1}^{N}\frac{1}{2}[1 + m\cos(2\pi n\xi/L) + \phi_n] \tag{11}$$

According to the superposition principle, the reconstructed field intensity is

$$I_N(\xi, z_1) = \left|\sum_{n=1}^{N} U_n(\xi, z_1)\right|^2 \tag{12}$$

$$= \sum_{n=1}^{N}|U_n|^2 + \sum_{n=1}^{N}\sum_{m=1}^{N} U_n U_m^*(1-\delta_{n,m}) \tag{13}$$

Due to the random phase term ϕ_n, the first term in Eq. (13) and the last term are independent random variables. Using the property that $\sigma^2(a+b) = \sigma^2(a) + \sigma^2(b)$ if a and b are independent random variables, we can write the variance of the reconstructed field intensity as:

$$\sigma^2(I_N) = \sum_{n=1}^{N}\sigma^2\left(|U_n|^2\right) + \sigma^2\left(\sum_{n=1}^{N}\sum_{m=1}^{N} U_n U_m^*(1-\delta_{n,m})\right)\,, \tag{14}$$

We argue based on the independence of the random phase terms random phase term ϕ_n, that this can be approximated as a linear sum of Talbot curves (see Eq. (8)):

$$\sigma_N^2(z_1) = A + \sum_{n=1}^{N} B \cos\left(\frac{2\pi\lambda n^2(z_0+z_1)}{L^2}\right), \tag{15}$$

with A and B constants. In the next section we verify the validity of this approximation in a simulation. Equation 15 provides a physical understanding of the width of the focus curve. The sum of cosines gives rise to a peak at $z_1 = -z_0$, the virtual image plane. For larger N, either because of a larger numerical aperture or more spatial spatial frequencies in the input, the peak width becomes smaller. The result in Eq. (15) gives a limit for the precision that can be achieved by depth from focus digital holography in terms of the peak width. In Fig. 1, the focus curve Eq. (15) in this ideal case is plotted as a function of reconstruction distance. In a real case scenario the peak is broadened, as in the preceding analysis starting from Eq. (11) it is assumed that the object has an ideal flat power spectrum, and the phases ϕ_n for spatial frequencies n/L were assumed to be statistically independent (ideal white noise input). For a real object the spatial frequency distribution of the object may be less ideal leading to less terms contributing to the summation in 15 and therefore resulting in a wider peak. Finally, the summation is limited by the numerical aperture and sampling of the imaging system. When the recording distance equals the critical sampling distance, the maximum spatial frequency that can be imaged is equal to the Nyquist frequency

$$\frac{N_{max}}{L} = \frac{1}{2\Delta\xi}, \tag{16}$$

and in the summation of Eq. (15) this limits the DFF-DH peak width.

3. SIMULATION

We compare a well-known method of Fresnel diffraction calculations, namely the transfer function approach, with the analytic model of Eq. (15). For background information and actual code we refer the reader to the work of Voelz (2011).[8] The input image in the simulation is given by Eq. (11), where the input object support L is 200 pixels, the number of pixels in the recording plane is N=1000, the number of unique spatial frequencies in the input image is $L/2-1$, the wavelength λ=633 nm, the pixelsize $\Delta\xi$=6.45 microns and the recording distance z_0 at $N\Delta\xi^2/\lambda$ (critical recording distance). These are parameters used in a typical experimental realization. The variance as a function of reconstruction distance is shown in Fig. 1. The simulated focus curve describes the analytic model of Eq. (15) well around the centre $z_1 = z_0$, and deviates towards the edges due to finite aperture effects that occur in the simulation, but are not accounted for in the analytic model. Both approaches lead to the same focus curve peak-width of approximately 450 microns, indicating the possibility of sub-mm axial resolution with DFF-DH without magnification.

4. MATERIALS AND METHODS

4.1 Setup

The digital holography setup is shown in Fig. 2 and consists of a Michelson interferometer in order to illuminate the object normal to the surface. No lenses or objectives are used in the imaging process, except to expand and collimate the illuminating laser beam to a width (FWHM) of approximately 1.5 cm. The object was placed approximately 7 cm away from the sensor plane. The light source is a HeNe laser with a wavelength of 633 nm and an output power in the order of 3 mW. The mirror in the reference arm is mounted onto a piezoelectric transducer controlled by a computer for phase-shifting digital holography, where we capture four holograms with a phaseshift of $\pi/2$ of the reference beam between each subsequent hologram. In this way we can use the full image plane and maximize the lateral resolution in the reconstructed image. The digital holograms were captured by a CCD camera (ORCA ER, Hamamatsu) with 1344 x 1024 pixels with a pixel size of 6.45 microns.

4.2 Sample

We use a brass reflector with a rough surface (obtained by briefly sandblasting the object) as a test target to demonstrate sub-mm axial resolution. The total area of the square sample is 25 mm^2. We characterise the surface using a white light interferometer (WLI, Bruker ContourGT-K). The measured roughness parameters S_a (average roughness) and S_q (root mean square roughness) are 3.571 microns and 11.597 microns respectively.

4.3 Digital holographic reconstruction

Even though the lateral sample dimensions are smaller than the sensor and thus the transfer function approach can be used, there is the possibility of the sample holder (which extends to beyond the sensor plane) appearing in the reconstructed image. Reconstruction of the digital holograms was performed using the S-FFT method[9] for this reason, since it does not restrict the reconstruction plane to the dimensions of the sensor.

5. RESULTS

Figure 3 shows a focus metric curve obtained from the experimental data. The experimental curve has a full width at half maximum of approximately 750 microns, which is significantly broader than the width of the simulated curve in Fig. 1 which has a width of around 200 microns. We attribute this to the fact that the frequency content of the object is not constant. In that sense, Fig. 1 represents a limiting case with uniform spatial frequency power spectrum in the input image. The spatial frequency content of the experimental input is estimated by taking the Fourier transform of the optimal in focus intensity image. The logarithm of the power spectrum in Figure 4 shows that indeed the power spectrum is not flat, but instead shows a significant drop off in power for high spatial frequencies.

6. CONCLUSIONS

We argued that the DFF curve as a function of reconstruction depth can be approximated by the sum of Talbot curves for every spatial frequency. Analytic theory and numerical simulation verified this approximation and indicated that the axial precision in terms of the peak width can be brought down to well below the millimeter range using a basic digital holography setup without imaging optics and magnification. Finally, we showed that sub-mm axial resolution is indeed possible based on a focus curve calculated from experimental data.

REFERENCES

[1] Leach, R., [*Optical Measurement of Surface Topography*], Springer Berlin Heidelberg (2011).

[2] Tachiki, M. L., Itoh, M., and Yatagai, T., "Simultaneous depth determination of multiple objects by focus analysis in digital holography," *Appl. Opt.* **47**, D144–D153 (Jul 2008).

[3] Ma, L., Wang, H., Li, Y., and Jin, H., "Numerical reconstruction of digital holograms for three-dimensional shape measurement," *Journal of Optics A: Pure and Applied Optics* **6**(4), 396 (2004).

[4] [*Digital Holography*], 41–69, Springer Berlin Heidelberg, Berlin, Heidelberg (2005).

[5] Tian, Y., Shieh, K., and Wildsoet, C. F., "Performance of focus measures in the presence of nondefocus aberrations," *J. Opt. Soc. Am. A* **24**, B165–B173 (Dec 2007).

[6] Subbarao, M. and Surya, G., "Depth from defocus: A spatial domain approach," *International Journal of Computer Vision* **13**, 271–294 (1994).

[7] Goodman, J., [*Introduction to Fourier Optics*], MaGraw-Hill, 2nd ed. (1996).

[8] Breckinridge, J. and Voelz, D., [*Computational Fourier Optics: A MATLAB Tutorial*], SPIE Press monograph, Society of Photo Optical (2011).

[9] Verrier, N. and Atlan, M., "Off-axis digital hologram reconstruction: some practical considerations," *Appl. Opt.* **50**, H136–H146 (Dec 2011).

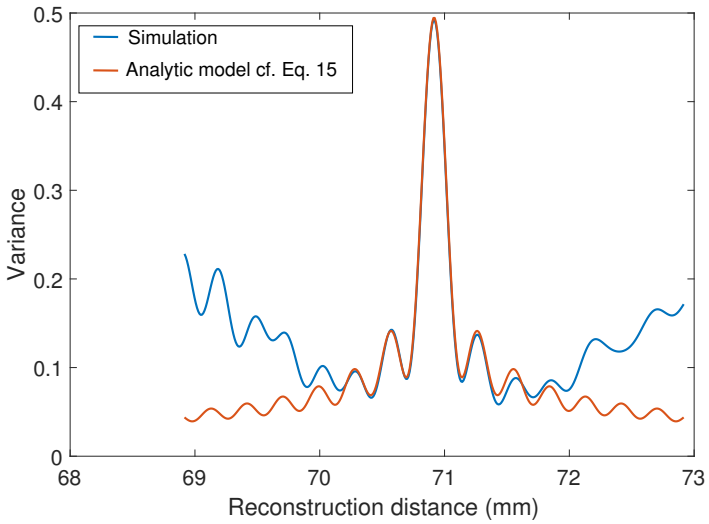

Figure 1. Comparison between the focus (variance) curves resulting from the Fresnel diffraction simulation (blue) and the analytic model Eq.15 (red). The difference between the two is due to the finite aperture used in the simulation. .

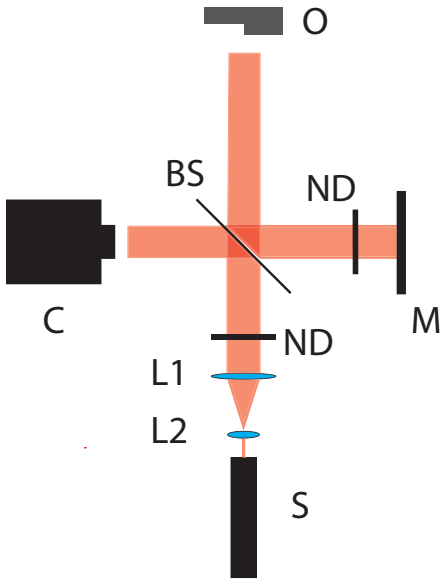

Figure 2. Michelson interferometer setup for acquiring the digital holograms. S=HeNe laser (633 nm), BS=pellicle beam-splitter, C=CCD camera (1344x1024 pixels), M=piezo mounted mirror and O=object, L=lens, ND=variable neutral density filter.

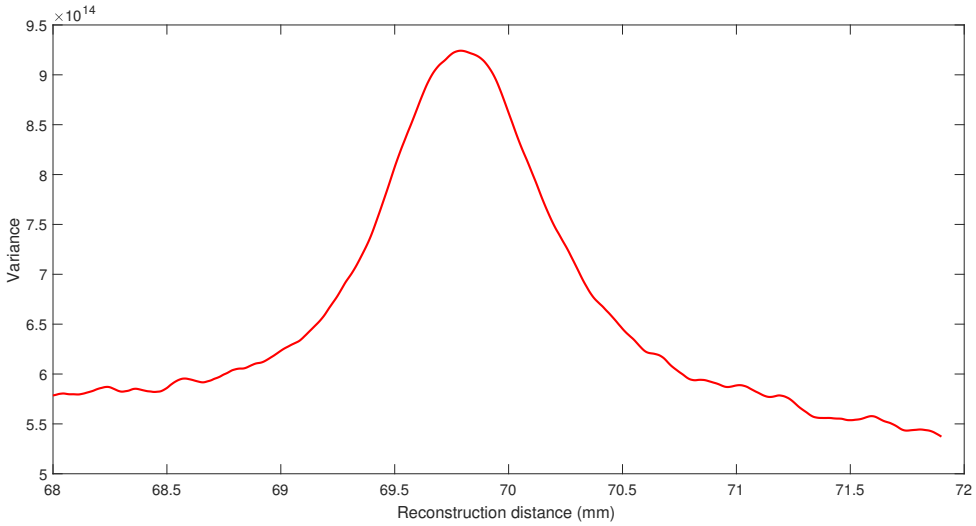

Figure 3. DFF-DH focus metric curve obtained from experimental data for a planar surface.

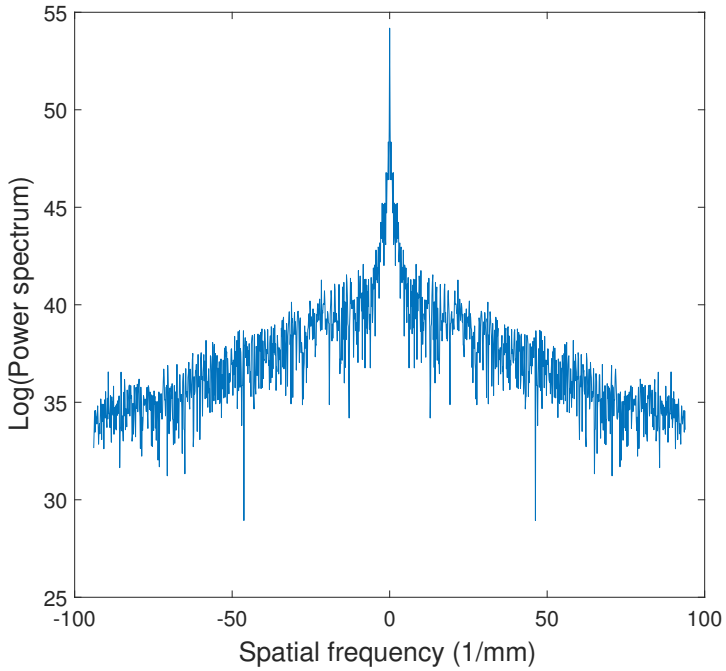

Figure 4. Logarithm of the object image power spectrum when reconstructed in focus. In contrast to what is assumed in DFF-DH the power spectrum is not flat.